

ACIDOSIS (MEASURED BY NUCLEAR MAGNETIC RESONANCE) AND ETHANOL PRODUCTION IN ANOXIC GOLDFISH ACCLIMATED TO 5 AND 20°C

BY AREN VAN WAARDE*, INGRID DE GRAAFF,
GUIDO VAN DEN THILLART AND CEES ERKELENS

*Departments of Biology (Animal Physiology) and Organic Chemistry,
Gorlaeus Laboratories, Leiden University, PO Box 9502, 2300RA Leiden,
The Netherlands*

Accepted 20 March 1991

Summary

Goldfish acclimated to 20 and 5°C were subjected to anoxia (3 h at 20°C and 18 h at 5°C). The intracellular pH (pHi) and the levels of high-energy phosphate compounds in the epaxial muscle were continuously monitored by *in vivo* ³¹P-n.m.r. spectroscopy. Free [ADP] was calculated from n.m.r.-measured reactants of the creatine kinase reaction and the creatine kinase equilibrium constant. A rapid initial drop in pHi was followed by a sudden decrease in the rate of development of acidosis. Similar biphasic time courses were observed for the increases in the levels of free ADP and inorganic phosphate and the decrease in phosphocreatine concentration.

In a parallel series of experiments, fish were placed in the flow cell of the n.m.r. probe (outside the magnet) and anesthetized after different anoxic intervals. Metabolites in red muscle, white muscle and blood were then assayed, using classical biochemical techniques. The transition to a less rapid decline in pH appears to be primarily due to a suppression of energy demand and activation of H⁺ extrusion; ethanol production becomes significant only after longer periods of anoxia. Anoxic exposure has no influence on the kinetic properties of muscle alcohol dehydrogenase, but acclimation of goldfish to low temperature increases alcohol dehydrogenase activity in white muscle.

Introduction

Goldfish [*Carassius auratus* (L.)] and crucian carp (*Carassius carassius* L.) can survive very long periods of environmental anoxia. The half-maximal survival time (LT₅₀) ranges from 16 h at 20°C (Van den Thillart, 1977) to several weeks and even months at temperatures below 5°C (Walker and Johansen, 1977; Van den Thillart

* Present address: PET Center, Academic Hospital, Groningen University, PO Box 30.001, 9700RB Groningen, The Netherlands.

Key words: *Carassius auratus*, *in vivo* ³¹P-n.m.r. spectroscopy, intracellular pH, high-energy phosphate compounds, anoxia.

et al. 1983; Holopainen and Hyvärinen, 1985; Piironen and Holopainen, 1986). The animals rely on a complex strategy for anoxic survival, consisting of a suppression of energy demand (Van Waversveld *et al.* 1988, 1989a,b) and a switch to a modified metabolism with ethanol, CO₂ and NH₃ as anaerobic end products (Van den Thillart and Kesbeke, 1977; Shoubridge and Hochachka, 1980; Van Waarde, 1983, 1988; Van Waversveld *et al.* 1989a,b).

Recently, we developed a flow-through probe for *in vivo* ³¹P-n.m.r. spectroscopy of fish (Van den Thillart *et al.* 1989a). The responses of intact animals to anoxia could be evaluated by means of this probe (Van den Thillart *et al.* 1989b; Van Waarde *et al.* 1990). We used three species with different strategies for anoxic survival: carp (*Cyprinus carpio*, classical Embden–Meyerhof glycolysis), tilapia (*Oreochromis mossambicus*, classical glycolysis plus metabolic suppression) and goldfish (*Carassius auratus*, modified glycolysis plus metabolic suppression). The initial rapid rate of development of acidosis in goldfish suddenly declined after the environmental water had been bubbled with nitrogen for 30 min at 20°C. In contrast, carp rapidly developed a severe acidosis. Tilapias switched to a lower rate of decline in pH after a short anoxic interval, but the contrast with the initial rapid fall was not as strong as that observed in goldfish (Van Waarde *et al.* 1990). Anaerobic end products were not measured in these studies, so the correlation between metabolism and n.m.r.-observed pH changes remained unknown.

Here we present ³¹P-n.m.r. observations on the responses to anoxia of goldfish acclimated to high (20°C) and low (5°C) temperature. In a parallel series of experiments, the animals were placed in the flow cell of the n.m.r. probe, subjected to anoxia and anesthetized after various anoxic intervals. Several key metabolites were assayed in the tissues after perchloric acid extraction, so that alterations in the n.m.r. spectra could be related to changes in the concentrations of metabolites. The red and white myotomal muscles were homogenized in sucrose buffer for the assay of alcohol dehydrogenase.

The experiments were performed to test the following hypotheses: (i) removal of glycolytically produced lactate by the ethanol-producing system is an important mechanism underlying the n.m.r.-observed dampening of acidosis; (ii) at 20°C, the energy demand of the animals is greater than the maximal flux through the ethanol pathway, so that lactate accumulates and there is a continuous decline in the intracellular pH. At low temperature, the energy demand and the capacity of the ethanol route are better matched, resulting in complete stabilization of intracellular pH after a short anoxic interval.

In addition, we tried to collect information about metabolic signals that might trigger the switch from lactate production to ethanol formation in the anoxic goldfish.

Materials and methods

Animals

Goldfish (*Carassius auratus*, comet tail variety) were used in all experiments.

The animals (body mass 80–100 g) were acquired from a commercial fish dealer. They were acclimated to a 12 h light period and temperatures of 5 or 20°C for at least 3 months. All fish were fed daily with trout food in pellet form (Trouvit^R, Trouw, Putten, The Netherlands).

In vivo ³¹P-n.m.r. spectroscopy

The n.m.r. experiments were carried out as described previously (Van den Thillart *et al.* 1989a,b; Van Waarde *et al.* 1990), using a Bruker MSL-400 spectrometer. The animals were restrained by an inflatable plastic bag which immobilized the myotome but left the head and gill covers free. They were held in an upright position within a flow cell and water was pumped over their gills through a flexible tube placed in their mouth. The ³¹P-n.m.r. signal of the epaxial muscle was picked up with an 18 mm surface coil, which was double-tuned to the frequencies of phosphorus (162 MHz) and protons (400 MHz) and was located about 20 mm behind the gill cover above the lateral line. A microsphere, filled with a solution of methylene diphosphonate in D₂O, was mounted at the center of the coil and served as an external intensity standard. The homogeneity of the stationary magnetic field was optimized by making the n.m.r. signal of the protons of intracellular water maximal. Fully relaxed ³¹P-n.m.r. spectra were accumulated over periods of 10 min and consisted of 136 individual scans, using a pulse width of 60°, an acquisition time of 0.4 s and a 4 s relaxation delay. The intracellular pH was calculated from the difference in chemical shift between the inorganic phosphate and phosphocreatine resonances in the n.m.r. spectra. The pH measurements were standardized using different model solutions (see Van den Thillart *et al.* 1989b). Spectra were acquired continuously before, during and for several hours after a period of environmental anoxia caused by bubbling the perfusion medium with nitrogen (Fig. 1). Anoxia was reached 30 min (20°C) or 60 min (5°C) after the gas phase had been switched from air to nitrogen. The onset of anoxia was defined as the moment when the water perfusing the gills produced the same oxygen electrode reading as a solution of 10 % sodium sulphite. Similarly, 100 % air saturation was reached 30 min (20°C) or 60 min (5°C) after the atmosphere had been changed from nitrogen to air. Removal of all oxygen from the water (and reoxygenation) took longer at the lower temperature because of the greater solubility of O₂ and the limited capacity of the gassing system. Each animal served as its own control and recovered completely after the reintroduction of air; there was no subsequent mortality.

Tissue extraction

In a parallel series of experiments, goldfish were placed in the flow cell of the bioprobe (outside the n.m.r. magnet). Water was pumped over their gills as in the n.m.r. studies. After various anoxic intervals, the animals were anesthetized by adding MS 222 to the water to a final concentration of 100 p.p.m. When anesthesia was complete, the fish were removed from the flow cell.

A 0.2 ml blood sample was drawn by cardiac puncture. The blood was weighed

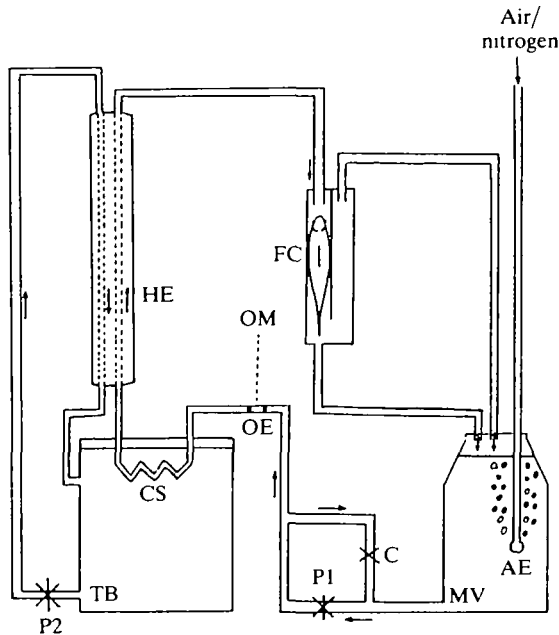


Fig. 1. Schematic drawing of the apparatus used in the experiments. AE, aerator (using either air or nitrogen); C, clamp (to adjust the water flow); CS, cooling spiral (stainless steel); FC, flow cell (fitted in the Bruker ^{31}P -bioprobe, which holds the animal); HE, heat exchanger (countercurrent principle, 90% of the length of the tube carrying water to the animal to avoid heating during transport); MV, mixing vessel (for water); OE, oxygen electrode; OM, oxygen meter; P1, Eheim aquarium pump; P2, Haake pump (belonging to the thermostatted bath); TB, thermostatted bath (Haake F3C, with heating and cooling unit, digital temperature read-out and proportional temperature regulation). All tubing was made of butyl rubber to minimize oxygen diffusion.

and 2 vols of 6% HClO_4 was added. The sample was homogenized on a Vortex mixer and temporarily stored on ice. Processing of the blood was completed within 3 min. The animal was then killed by decapitation. After removal of the scales and skin, the red and white muscles of the right myotome were rapidly excised, freeze-clamped and extracted with 8% (w/v) HClO_4 , 40% (v/v) ethanol, 4 mmol l^{-1} NaF, 10 mmol l^{-1} EDTA, as described previously (Van den Thillart *et al.* 1982, 1990). After neutralization with 2 mol l^{-1} K_2CO_3 and removal of KClO_4 by centrifugation, the supernatant was used for metabolite assays.

The myotomal muscles of the left-hand side of the animal were excised, cut into small pieces, weighed and homogenized in 10 vols of 250 mmol l^{-1} sucrose, 20 mmol l^{-1} Tris-Cl, 10 mmol l^{-1} Hepes and 1 mmol l^{-1} EGTA (pH 7.4), using a Potter-Elvehjem homogenizer with a Teflon pestle. After centrifugation (15 min, 10 000 g), the supernatant was used to determine the activity of alcohol dehydrogenase.

Protein in the blood sample was removed by centrifugation (5 min, Eppendorf

centrifuge). The supernatant was neutralized with K₂CO₃, recentrifuged to remove KClO₄ and used for enzymatic determination of ethanol.

Metabolite measurements

Ethanol, lactate and ammonia were determined with commercial test kits (Boehringer Mannheim, BRD). Pyruvate and α -ketoglutarate were assayed according to Williamson *et al.* (1967) and phosphocreatine, ATP and glutamate by standard procedures described in Bergmeyer (1970).

Alcohol dehydrogenase assay

Alcohol dehydrogenase activity was measured as ethanol formation. The reaction mixture contained 188 mmol l⁻¹ sucrose, 15 mmol l⁻¹ Tris-Cl, pH 7.4, 7.5 mmol l⁻¹ Hepes, 0.8 mmol l⁻¹ EGTA, 0.2 mmol l⁻¹ NADH and 0.05–10 mmol l⁻¹ acetaldehyde in a volume of 1.2 ml (Mourik *et al.* 1982). The activity at saturating substrate concentration (V_{\max}) and the affinity of the enzyme for its substrate (K_m) were estimated from Lineweaver–Burke plots. These consisted of six data points with correlation coefficients of 0.995 or more.

Statistical treatment of data

The biphasic data for the development of acidosis and phosphocreatine utilization were analyzed with a special computer program which searches for transition points (Yeager and Ultsch, 1989). Differences between groups were checked using the non-parametric test of Wilcoxon. Differences of $P < 0.05$ were considered statistically significant.

Results

Development of acidosis

At both environmental temperatures, goldfish developed an acidosis in the absence of oxygen. The pattern of pH changes is illustrated in Fig. 2. When the gas phase was switched from air to nitrogen, there was a short lag (10 min at 20°C, 80 min at 5°C) during which the pHi of the myotome did not change. The lag was followed by a steep decline in the intracellular pH. After a certain interval (54 min of N₂ bubbling at 20°C, 138 min at 5°C, i.e. after the onset of anoxia), the rate of increase in acidosis suddenly declined and the pH continued to fall more slowly, at a rate that was maintained for the remainder of the anoxic period. It is therefore possible to distinguish initial and final rates of decline in pH. We call the moment of 'dampening' of the development of acidosis the *transition time*.

Table 1 presents a statistical treatment of the n.m.r. data. The normoxic pHi of the myotomal muscle was higher in animals acclimated to 5°C than in those maintained at 20°C. The pH values at the transition time and at the time when phosphocreatine stores were depleted by half were also higher in cold-acclimated fish. The initial rate of development of acidosis was 2.5 times lower at the lower temperature and the final rate of pH decline was 11 times lower. The dampening of

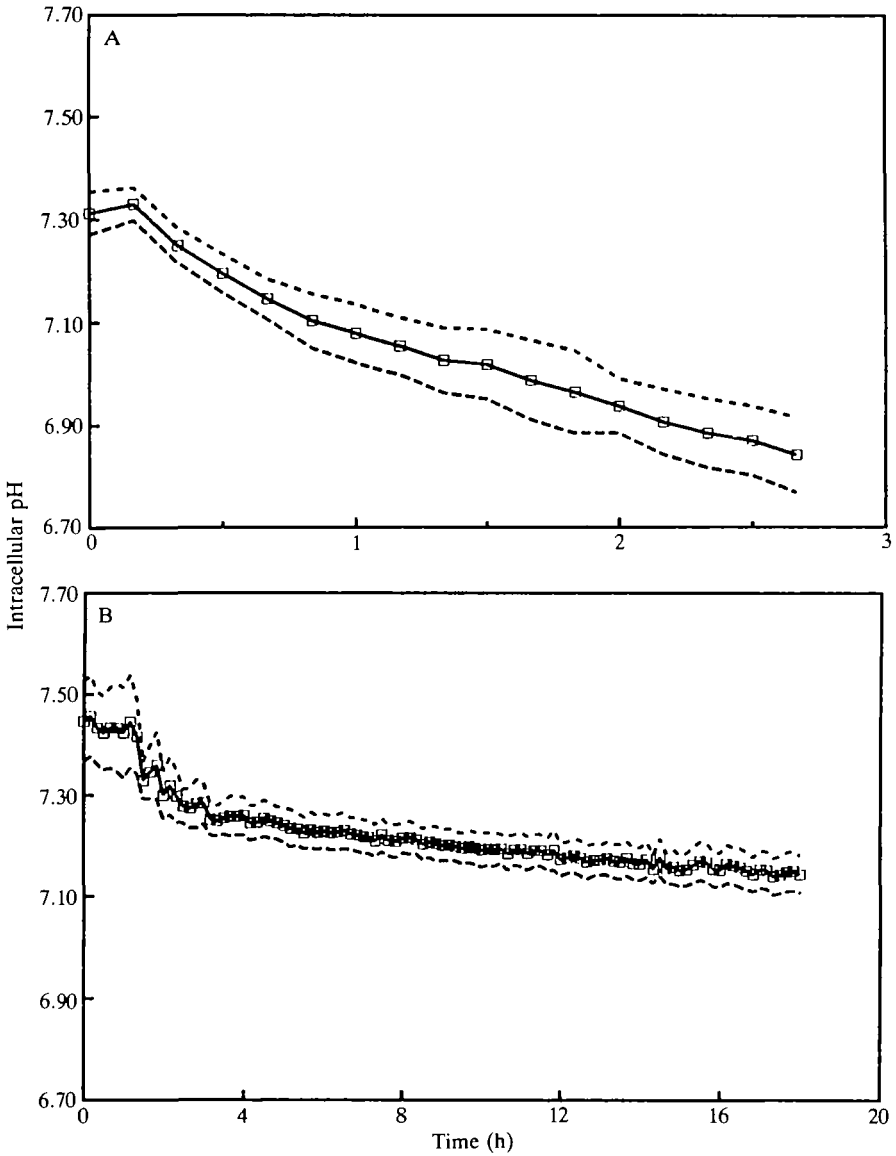


Fig. 2. Development of acidosis in anoxic goldfish acclimated to 20°C (A) and 5°C (B). Time zero corresponds to the onset of nitrogen bubbling of the ambient water. Note the different time scales at the two temperatures. The means \pm standard errors for seven (20°C) and five (5°C) different animals are indicated.

acidosis (defined as the initial rate of decline in pH/the final rate) was thus much greater in cold-acclimated animals.

Phosphocreatine utilization

The pattern of phosphocreatine (PCr) utilization is illustrated in Fig. 3. In fish

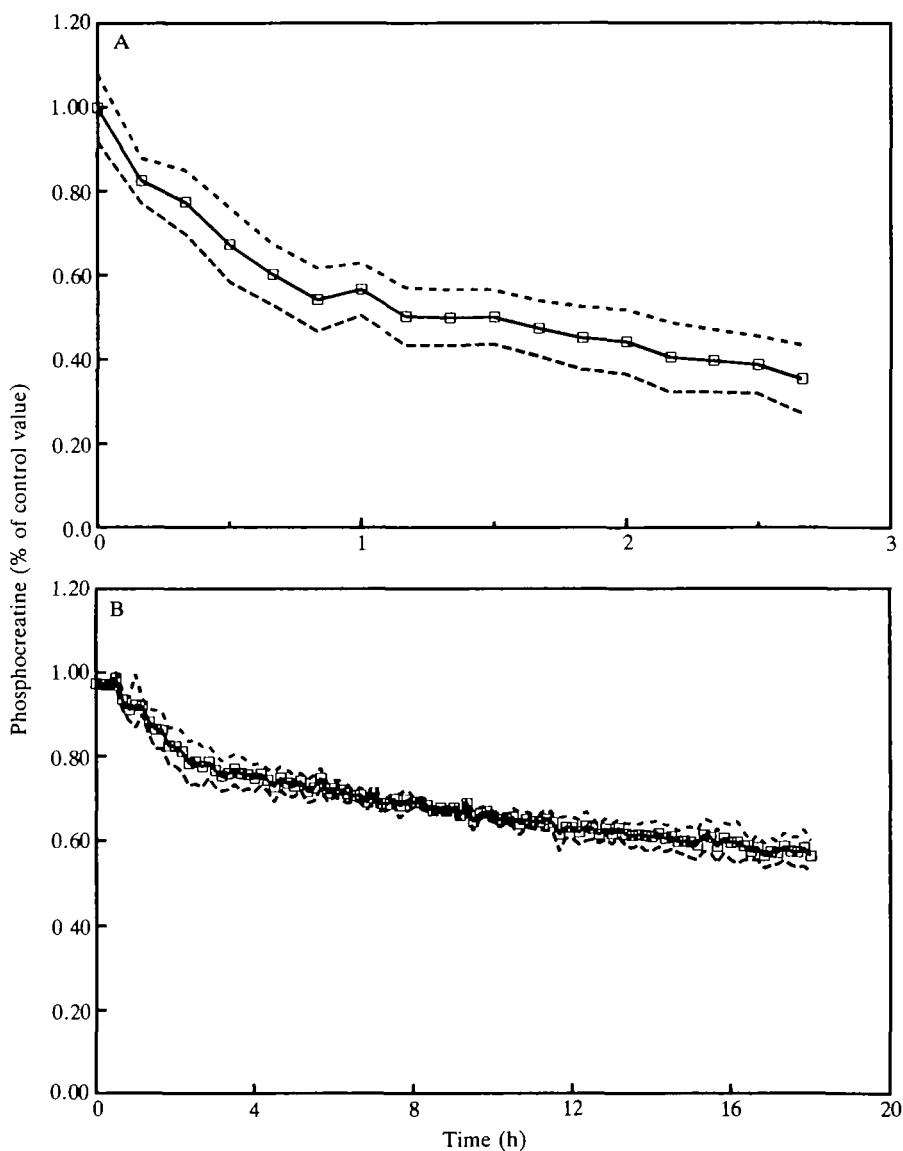


Fig. 3. Phosphocreatine utilization in anoxic goldfish acclimated to 20°C (A) and 5°C (B). Time zero corresponds to the onset of nitrogen bubbling of the ambient water. Note the different time scales at the two temperatures. The means \pm standard errors for seven (20°C) and five (5°C) different animals are indicated; [PCr] is expressed as a fraction of the control value.

acclimated to 20°C, the PCr concentration declined immediately in response to reduced oxygen availability, whereas there was a lag of 30–40 min at 5°C. After an interval (38 min of N₂ bubbling at 20°C, 132 min at 5°C, i.e. after the onset of anoxia), PCr demand was reduced and the phosphagen reserve was further

Table 1. Development of acidosis in muscle of anoxic goldfish

Condition	Normoxic pHi	Transition pHi	Transition time (min of N ₂ bubbling)		pHi at 50 % PCr depletion	Initial rate of pH decline (pH units min ⁻¹ ×10 ³)	Final rate of pH decline (pH units min ⁻¹ ×10 ³)	Dampening of acidosis
			Transition pHi	Transition time				
5°C-acclimated	7.49±0.03	7.33±0.07	138±51	7.16±0.03	2.92±1.28	0.15±0.07	23.2±13.9	
20°C-acclimated	7.32±0.03	7.11±0.07	54±25	7.01±0.05	7.00±3.50	1.68±1.23	4.0±1.2	
	<i>P</i> <0.01	<i>P</i> <0.01	<i>P</i> <0.05	<i>P</i> <0.01	<i>P</i> <0.05	<i>P</i> <0.01	<i>P</i> <0.01	

Means±s.d. of five (5°C) or seven (20°C) different animals.
 All values were obtained by *in vivo* ³¹P-n.m.r. spectroscopy.
P is a dual-tail probability (Wilcoxon's *Q*-test).
 * Initial rate of pH decline/final rate of pH decline.
 PCr, phosphocreatine.

Table 2. Net phosphocreatine utilization in muscle of anoxic goldfish

Condition	Transition [PCr] (% of control)	Transition time (min of N ₂ bubbling)	Initial rate (% of control min ⁻¹)	Final rate (% of control min ⁻¹)	Suppression of PCr demand*
5°C acclimated	84±8	132±55	0.41±0.38	0.02±0.01	21.1±15.0
20°C acclimated	61±13	38±11	1.57±0.69	0.17±0.09	9.4±3.8
	<i>P</i> <0.05	<i>P</i> <0.05	<i>P</i> <0.05	<i>P</i> <0.01	NS

Means±s.d. of five (5°C) or seven (20°C) different animals.
 All values were obtained by *in vivo* ³¹P-n.m.r. spectroscopy.
P is a dual-tail probability (Wilcoxon's *Q*-test); NS, not significant.
 * Initial rate of PCr utilization/final rate of PCr utilization.

depleted at a low rate that was maintained for the rest of the anoxic period. It is therefore possible to distinguish initial and final rates of PCr utilization, before and after the transition time.

Table 2 presents a statistical analysis of the n.m.r. data. The initial rate of depletion of the phosphagen stores was about four times lower at 5°C than at 20°C, and the final rate of PCr utilization was 8.5 times lower. The suppression of PCr demand (defined as the initial rate of PCr utilization/the final rate) appeared to be greater in cold-acclimated fish, but this tendency was not statistically significant, owing to large individual variability.

Changes in inorganic phosphate concentrations

The time course of changes in the myotomal inorganic phosphate (Pi) concentration during a period of oxygen deficiency is illustrated in Fig. 4. Phosphocreatine utilization appeared to result in the accumulation of inorganic phosphate. Pi increased immediately in animals acclimated to 20°C and after a lag of 40 min in animals acclimated to 5°C. The steep rise in the Pi level came to an end after 40 min of N₂ bubbling at 20°C and 140 min at 5°C, i.e. after the onset of anoxia. Pi then continued to be produced at a low rate that was maintained for the rest of the anoxic period.

Changes in ATP concentration

As shown in Fig. 5, the intracellular ATP concentration was well stabilized at both environmental temperatures. The decline in [ATP] was less than 15% after 3 h of oxygen deficiency at 20°C and about 10% after 18 h of anoxia at 5°C.

Changes of free ADP concentration in the sarcoplasm

We calculated free [ADP] in the sarcoplasm from n.m.r.-measured concentrations of [ATP], [PCr] and [H⁺], chemically determined [total creatine] and [ATP], and the creatine kinase equilibrium constant, as discussed previously (Van Waarde *et al.* 1990). Time courses of changes in [free ADP] are depicted in Fig. 6. Nitrogen bubbling induced an immediate increase in [ADP] at both acclimation temperatures, but the steep rise in the ADP concentration ended after 35 min at 20°C and 110 min at 5°C, i.e. after the onset of anoxia. The ADP level continued to increase at a low rate that was maintained for the rest of the anoxic period.

Accumulation of anaerobic end products

The concentrations of some key metabolites and anaerobic end products in lateral red muscle, epaxial white muscle and blood are presented in Table 3. The ethanol level in normoxic animals was very low. At the transition time (0.8 h at 20°C, 3 h at 5°C), ethanol concentrations showed slight, but significant, increases. At the end of the anoxic period, the ethanol concentration was 1.5–2 mmol l⁻¹.

Lactic acid accumulated in both muscle types during anoxia. The lactate/pyruvate concentration ratio of red muscle was significantly increased at the transition

Table 3A. *Enzyme activities and metabolite levels in goldfish acclimated to 5°C*

	Normoxic controls (N=4)	Transition (3 h of N ₂) (N=4)	Anoxia (18 h of N ₂) (N=4)
Blood			
[Ethanol]	0.07±0.02	0.24±0.03*	1.87±0.80*
Red muscle			
ADH, V _{max}	43.3±4.6	55.7±10.3	37.6±10.5
ADH, K _m	0.24±0.10	0.31±0.12	0.19±0.04
[Lactate]	2.42±0.67	4.73±0.98*	5.65±0.55*
[Pyruvate]	0.05±0.02	0.05±0.01	0.05±0.02
[Lactate]/[pyruvate]	54±11	97±10*	159±90*
[Glutamate]	2.69±0.90	2.38±0.19	2.63±0.81
[α-Ketoglutarate]	0.04±0.03	0.05±0.03	0.03±0.03
[NH ₄ ⁺]	1.22±0.21	1.38±0.81	1.10±0.05
[Glu]/[αKG]·[NH ₄ ⁺]	88±39	36±17	86±54
[Phosphocreatine]	9.28±2.45	8.23±1.53	6.03±1.42
[ATP]	3.55±0.32	2.67±0.56	3.08±0.23
White muscle			
ADH, V _{max}	12.9±3.8	15.2±4.1	12.1±1.2
ADH, K _m	0.18±0.03	0.33±0.10	0.19±0.12
[Lactate]	2.32±0.40	3.19±0.47	5.21±1.28*
[Pyruvate]	0.05±0.03	0.04±0.01	0.01±0.01*
[Lactate]/[pyruvate]	56±29	78±38	415±113*
[Glutamate]	1.00±0.36	0.78±0.30	0.97±0.10
[α-Ketoglutarate]	0.02±0.01	0.01±0.01	0.02±0.03
[NH ₄ ⁺]	1.33±0.06	0.84±0.28	1.32±0.32
[Glu]/[αKG]·[NH ₄ ⁺]	53±21	69±29	36±16
[Phosphocreatine]	9.49±2.57	6.75±2.70	6.82±2.72
[ATP]	5.34±0.49	5.40±0.36	4.67±0.31

time (0.8 h of hypoxia at 20°C and 3 h of hypoxia at 5°C), but in white muscle this ratio increased only after prolonged periods of oxygen deficiency. No significant changes were observed in the concentrations of glutamate, α-ketoglutarate and NH₄⁺, or in the [glutamate]/[α-ketoglutarate]·[NH₄⁺] ratio. Muscle [ATP] was maintained well during anoxia, but phosphocreatine concentration declined markedly at 20°C.

Ethanol was undetectable in the ambient water, both at 5°C and at 20°C. The lack of measurable ethanol accumulation was not due to oxidation or evaporation, for internal standards added to the system were quantitatively recovered even after 48 h. Fish were absent during these tests, but the mixing vessel contained aquarium water bubbled with air or nitrogen.

Table 3B. Enzyme activities and metabolite levels in goldfish acclimated to 20°C

	Normoxic controls (<i>N</i> =3)	Transition (0.8 h of N ₂) (<i>N</i> =3)	Anoxia (3 h of N ₂) (<i>N</i> =3)
Blood			
[Ethanol]	0.20±0.06†	0.46±0.06*	1.56±0.36*
Red muscle			
ADH, V_{\max}	52.3±5.4	51.2±8.3	51.3±3.6
ADH, K_m	0.31±0.11	0.36±0.07	0.26±0.05
[Lactate]	3.19±0.03	4.94±1.10*	5.06±0.12*
[Pyruvate]	0.13±0.03†	0.09±0.02	0.03±0.02*
[Lactate]/[pyruvate]	25±6†	55±15*	170±80*
[Glutamate]	3.96±1.08	2.68±1.29	2.30±0.47
[α -Ketoglutarate]	0.01±0.02	0.03±0.00	0.01±0.02
NH ₄ ⁺	1.68±0.75	1.31±0.28	2.11±1.45
[Glu]/[α KG]·[NH ₄ ⁺]	175±85	75±40	77±55
[Phosphocreatine]	9.72±1.11	7.98±2.47	2.01±1.43*
[ATP]	4.59±0.70†	4.27±0.89	3.74±1.01
White muscle			
ADH, V_{\max}	6.4±1.6†	6.4±0.2	7.5±1.2
ADH, K_m	0.30±0.15	0.23±0.06	0.32±0.12
[Lactate]	1.43±0.42†	3.99±1.03*	7.00±1.19*
[Pyruvate]	0.11±0.01†	0.11±0.06	0.03±0.02*
[Lactate]/[pyruvate]	13±5†	38±28	250±180*
[Glutamate]	1.08±0.50	0.82±0.65	0.74±0.33
[α -Ketoglutarate]	0.01±0.00	0.02±0.01	0.01±0.01
[NH ₄ ⁺]	0.87±0.37†	1.55±0.39	1.75±0.71
[Glu]/[α KG]·[NH ₄ ⁺]	90±60	32±30	310±200
[Phosphocreatine]	12.3±3.2	4.48±0.75*	2.01±1.43*
[ATP]	5.69±1.37	5.65±1.31	5.52±0.22

Metabolite levels are presented as a mean±s.d. of *N* animals and expressed as $\mu\text{mol g}^{-1}$ wet mass.

Alcohol dehydrogenase (ADH) activities (V_{\max}) are expressed as $\mu\text{mol g}^{-1} \text{min}^{-1}$ at 25°C; affinities are in mmol l^{-1} acetaldehyde.

*Significant difference with respect to the normoxic control value ($P<0.05$); †significant difference between normoxic fish acclimated to 20°C and those acclimated to 5°C ($P<0.05$).

Glu, glutamate; α KG, α -ketoglutarate.

Kinetic properties of alcohol dehydrogenase

The activities of alcohol dehydrogenase in the myotomal muscles and the measured affinities of the enzyme for acetaldehyde are also presented in Table 3. The enzyme of red muscle had a higher V_{\max} than its counterpart in white muscle.

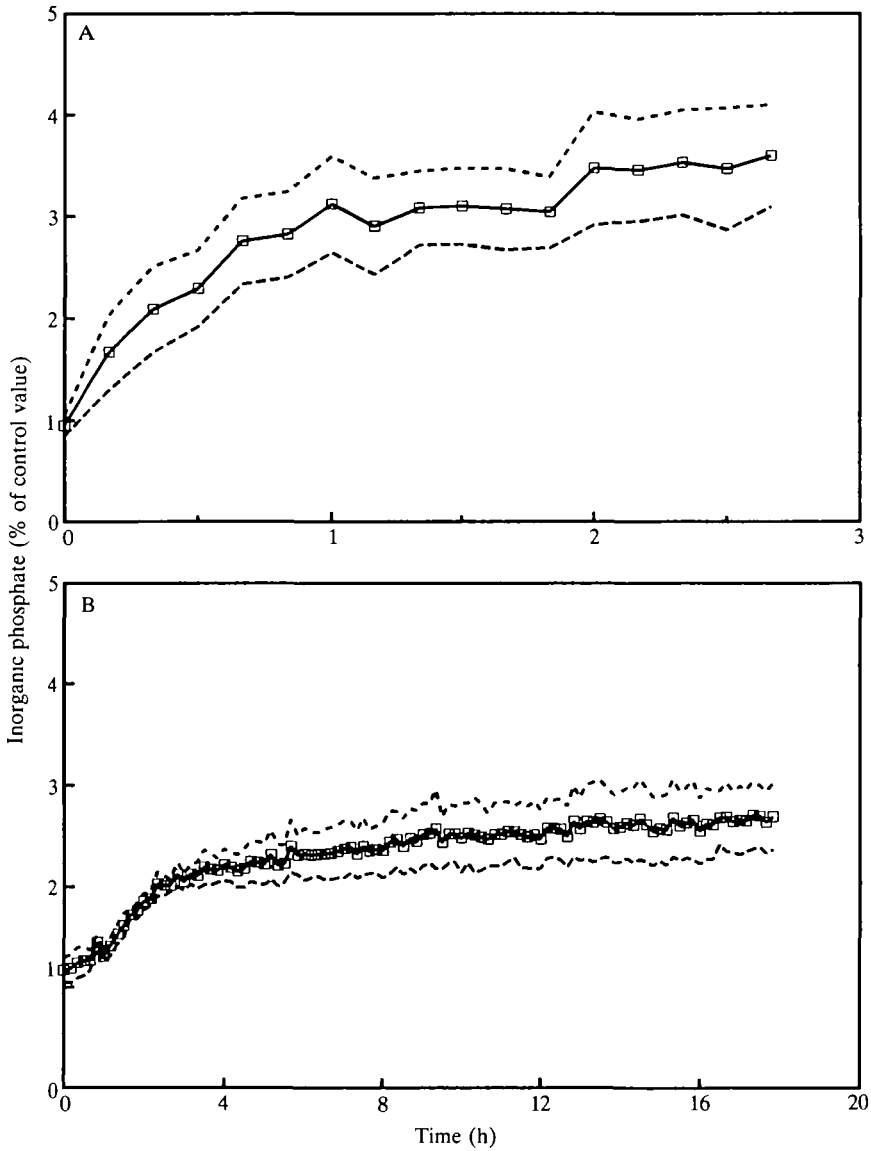


Fig. 4. Time course of changes in inorganic phosphate concentration in anoxic goldfish acclimated to 20°C (A) and 5°C (B). Time zero corresponds to the onset of nitrogen bubbling of the ambient water. Note the different time scales at the two temperatures. The means \pm standard errors of seven (20°C) and five (5°C) different animals are indicated; [Pi] is expressed as a fraction of the control value.

The differences were greater at 20°C than at 5°C, namely eightfold and threefold, respectively. In contrast, K_m values in the two muscle types were similar (0.18–0.36 mmol l⁻¹ at both environmental temperatures). Anoxic exposure did not induce significant changes in K_m or V_{max} .

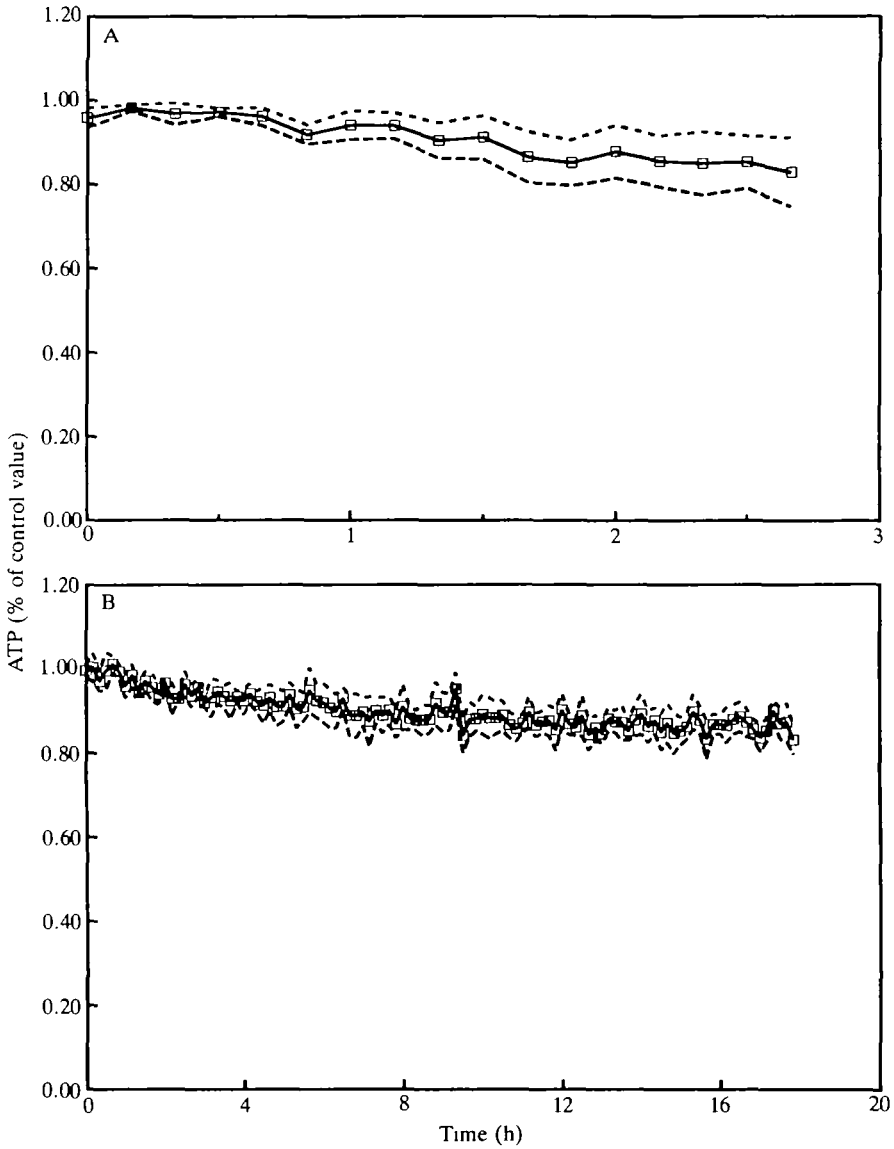


Fig. 5. Time course of changes in ATP concentration in anoxic goldfish acclimated to 20°C (A) and 5°C (B). Time zero corresponds to the onset of nitrogen bubbling of the ambient water. Note the different time scales at the two temperatures. The means \pm standard errors of seven (20°C) and five (5°C) different animals are indicated; [ATP] is expressed as a fraction of the control value.

Discussion

Metabolic events induced by oxygen deficiency

Figs 2–6 suggest the following sequence of events after the onset of nitrogen

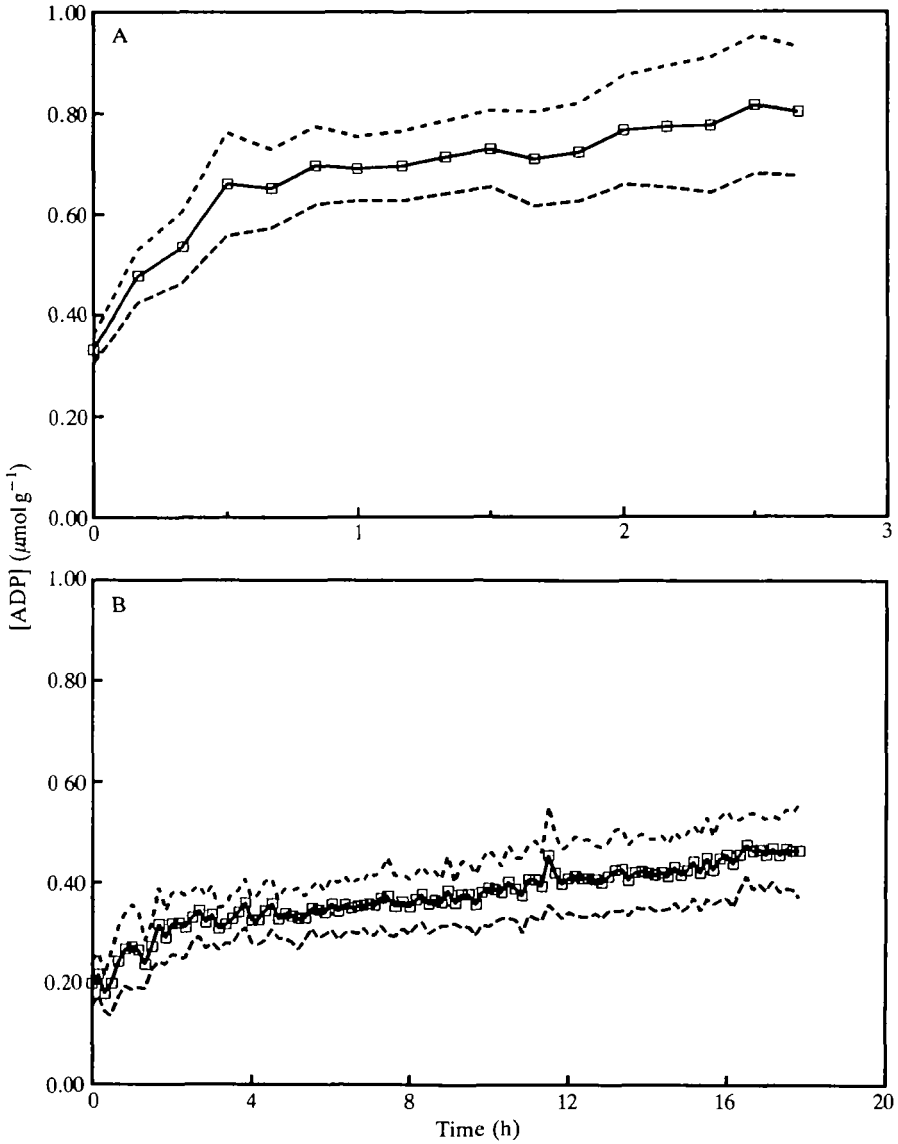
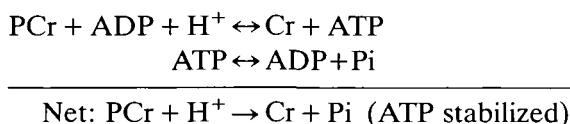


Fig. 6. Time course of changes in the concentration of free ADP in anoxic goldfish acclimated to 20°C (A) and 5°C (B). Time zero corresponds to the onset of nitrogen bubbling of the ambient water. Note the different time scales at the two temperatures. The means \pm standard errors of seven (20°C) and five (5°C) different animals are presented.

bubbling of the ambient water. The cytosolic level of ADP increases when the decline in P_{O_2} starts to limit the rate of oxidative phosphorylation. The rise in the concentration of free ADP induces a shift of the creatine kinase (CK) equilibrium in the direction of ATP formation, causing stabilization of [ATP] at the expense of

the phosphocreatine store. The decline in [PCr] is accompanied by the appearance of inorganic phosphate (see below):



The increases in [ADP] and [P_i] activate glycolysis by allosteric modulation of phosphofructokinase. When glucose has been broken down to the level of lactate, carbohydrate metabolism starts to generate protons (Pörtner, 1987). Since H⁺ is a substrate for creatine kinase, the resulting decline in the intracellular pH causes a further shift of the CK equilibrium and additional depletion of the phosphocreatine pool (Van Waarde *et al.* 1990).

Mechanisms underlying the 'dampening' of acidosis

After a certain anoxic interval, the rate of decline of pHi decreases (Fig. 2). This phenomenon could, in theory, be based on three different processes: (1) activation of the ethanol pathway, causing removal of lactate by lactate dehydrogenase, pyruvate decarboxylase and alcohol dehydrogenase and a diminished rate of acid production, since alcoholic fermentation does not generate protons, in contrast to lactate glycolysis (Pörtner, 1987); (2) a reduction in energy demand below the aerobic resting level, called 'metabolic arrest' by Hochachka (1982, 1985) and Hochachka and Guppy (1987), with a corresponding decrease in the glycolytic flux; (3) activation of transmembrane pH regulatory mechanisms, causing a more rapid efflux of protons from the myotome.

The hypothesis that the dampening of acidosis is due to activation of the ethanol pathway can be tested by measuring ethanol levels in anoxic fish and in the ambient water. As shown in Table 3, the transition to a low rate of acidification coincides with a slight, but significant, rise in the ethanol concentration in the blood. Thus, conversion of lactate to ethanol seems to contribute to the 'dampening' of acidosis. However, the accumulation of ethanol in the fish body is relatively minor (Table 3). The fourfold and 23-fold reductions in the rate of decline of pHi after the transition time (Table 1) should be associated with a switch from lactate to ethanol as the main anaerobic end product, if they are caused by a switch to alcoholic fermentation. In reality, lactate formation seems to predominate even after the transition time, for lactate accumulates in white muscle (the tissue monitored by n.m.r.) at 1.37 μmol g⁻¹ h⁻¹ at 20°C and 0.13 μmol g⁻¹ h⁻¹ at 5°C, whereas ethanol appears in the blood at 0.50 μmol g⁻¹ h⁻¹ at 20°C and 0.11 μmol g⁻¹ h⁻¹ at 5°C (Table 3). The rate of ethanol accumulation in the blood is not markedly increased after the transition. At 5°C, it accumulates at 0.06 μmol g⁻¹ h⁻¹ before and 0.11 μmol g⁻¹ h⁻¹ after the transition point. At 20°C, the corresponding values are 0.33 and 0.50 μmol g⁻¹ h⁻¹ (Table 3). Ethanol excretion appears to be negligible, because ethanol cannot be detected in the ambient water. Since ethanol accumulation in the fish body is relatively unimportant

ant and very little ethanol is excreted, a steady state for ethanol has not been reached and the ethanol pathway is incompletely activated under the conditions of this study. Thus, it is unlikely that the primary cause of the sudden transition to a less rapid decline in pH (Fig. 2) is a switch to alcoholic fermentation.

Information about the occurrence of metabolic suppression can be obtained from the rates at which end products (lactate, ethanol) accumulate and phosphorylated compounds (ATP, phosphocreatine) decline. As shown in Fig. 5, there is very little catabolism of ATP during the experiments, and no change in the rate of ATP depletion occurs at the transition time. In contrast, utilization of PCr is strongly suppressed after a short anoxic interval (Fig. 3; Table 2). The rate of lactate accumulation is also reduced after the transition. In white muscle of 5°C-acclimated fish, it is accumulated at $0.29 \mu\text{mol g}^{-1} \text{h}^{-1}$ initially and $0.13 \mu\text{mol g}^{-1} \text{h}^{-1}$ after the transition time. At 20°C, the corresponding values are 3.20 and $1.37 \mu\text{mol g}^{-1} \text{h}^{-1}$ (Table 3). The simultaneous reduction in the rates of utilization of phosphocreatine (Fig. 3), development of acidosis (Fig. 2) and accumulation of lactate (Table 3) suggests a suppression of energy demand.

The phenomenon of 'metabolic arrest' has been demonstrated by direct calorimetry of free-swimming goldfish by Van Waversveld *et al.* (1988, 1989*a,b*), but the time course of this process has not been established because of the large time constant of the measuring vessel. Figs 2–6 of the present paper suggest that energy demand remains high during the hypoxic period, but is lowered after the onset of anoxia.

However, comparison of the increase in [lactate] (Table 3) and the decline in intracellular pH (Table 1) indicates that 'metabolic arrest' is not the only cause of the n.m.r.-observed dampening of acidosis. The ratio of lactate accumulation rates before and after the transition point is $0.29/0.13=2.2$ at 5°C and $3.20/1.37=2.3$ at 20°C (Table 3, see above). In contrast, the fall in pH_i is dampened by factors of 23.2 at 5°C and 4.0 at 20°C (Table 1). The observation that lactate accumulation in white muscle is less strongly suppressed than is the accumulation of protons suggests an activation of transmembrane pH regulatory mechanisms in anoxic fish.

Regulation of the ethanol pathway

The measurements of alcohol dehydrogenase kinetics (Table 3) indicate that the properties of this enzyme are not altered by anoxic exposure. This finding contrasts with observations in plants, where anoxia generally induces a marked increase in V_{max} and the appearance of isozymes with a higher affinity for NADH or acetaldehyde (reviewed by Van Waarde, 1991). The ethanol pathway appears to be regulated at its rate-limiting step, the pyruvate decarboxylase reaction, which takes place in the mitochondria and is probably catalyzed by the pyruvate dehydrogenase (PDH) complex (Mourik *et al.* 1982; Van Waarde, 1991). Regulation of pyruvate decarboxylase (PDC) may involve both covalent and non-covalent mechanisms. The non-covalent mechanisms include modulation by cofactors (the NADH/NAD⁺ ratio) or allosteric effectors (ATP, ADP, Pi), product inhibition (by acetyl CoA) and substrate activation (by pyruvate),

whereas the covalent mechanism may involve hormonal signals and be based on PDH phosphorylation (Van den Thillart and Van Waarde, 1991). Regulation by the mitochondrial $[NADH]/[NAD^+]$ ratio seems unlikely, since no increase in the $[glutamate]/[\alpha\text{-ketoglutarate}] \cdot [NH_4^+]$ redox couple has been found in the present study or in previous work on free-swimming animals (Van den Thillart *et al.* 1982). Pyruvate concentrations in the myotome are not increased by anoxia (Table 3; Van den Thillart *et al.* 1982), so changes in pyruvate decarboxylase flux due to increased pyruvate availability are also ruled out. However, a regulating effect of the mitochondrial $[ATP]/[ADP] \cdot [Pi]$ ratio seems likely for the following reasons. (1) [free ADP] is increased twofold (Fig. 6) and [Pi] is increased 2.5- to threefold (Fig. 4) at the transition time. Since [ATP] is not changed significantly (Fig. 5), the $[ATP]/[ADP] \cdot [Pi]$ ratio is reduced five- to sixfold with respect to the normoxic control value. (2) In experiments involving goldfish muscle mitochondria, G. van den Thillart and M. Verhagen (unpublished results) observed that the anaerobic decarboxylation of pyruvate is modulated by the $[ATP]/[Pi]$ ratio. In the presence of 10 mmol l^{-1} Pi, PDC shows maximal activity. When 10 mmol l^{-1} ATP and no Pi are present, the rate is reduced to 15% of V_{\max} [in both cases, 0.1 mmol l^{-1} adenylylimidodiphosphate (AMPPNP) was added to inhibit ATPases]. Therefore, a decline in the phosphorylation potential seems to be one of the signals activating the ethanol pathway.

Effects of acclimation to low temperature

As shown in Table 1, the (n.m.r.-measured) intracellular pH of the epaxial white muscle is higher at 5°C than at 20°C . This observation was expected, since the acid-base balance is known to be temperature-dependent. The equilibrium constant (K_{eq}) of buffering systems changes with temperature, which causes a change in the intracellular pH. The change we found in our n.m.r. experiments ($0.17 \text{ pH units per } 15^\circ$, i.e. $-0.0113 \text{ pH units degree}^{-1}$) is very close to previously published values for white muscle of channel catfish (*Ictalurus punctatus*), based on estimations of pHi from the equilibrium distribution of a radiolabelled weak acid (Cameron and Kormanik, 1982).

Table 3 shows that the activity of alcohol dehydrogenase in red muscle is similar at both environmental temperatures. However, ADH activity in white muscle is significantly higher in 5°C -acclimated individuals than in fish acclimated to 20°C ($P < 0.01$, Wilcoxon's Q -test). This may indicate that the capacity for ethanol production in white fibers is increased by acclimation to low temperature.

In conclusion, the hypotheses mentioned in the Introduction have not been supported by the results of this study. The major reason for the (n.m.r.-observed) dampening of acidosis is not a switch to alcoholic fermentation. Acidosis is more strongly suppressed at low temperature, but even at 5°C the intracellular pH does not stabilize completely. We had expected such stabilization, since the blood of cannulated, anoxic crucian carp reaches a stable pH after a short anoxic interval (Van den Thillart and Van Waarde, 1991). It is possible to argue that in our goldfish a plateau would have been reached after a longer period, but it is equally

probable that the conditions in the n.m.r. probe (vertical position, confinement) cause an impaired resistance to anoxia. A comparison of the LT_{50} values of free-swimming and confined animals might enable us to choose between these two alternatives.

Though the benefits of the n.m.r. technique might be partially offset by the confinement stress that is imposed, certain interesting findings emerge from this study. (1) The initial response of the creatine kinase equilibrium to reduced oxygen availability is due to an increase in the concentration of free ADP, but the subsequent appearance of H^+ causes an additional shift towards ATP formation. The concentrations of ADP and H^+ both change by a factor 2.5 in the anoxic goldfish. (2) The n.m.r.-observed 'dampening' of acidosis appears to involve activation of H^+ extrusion besides metabolic suppression. (3) Anoxia does not induce novel alcohol dehydrogenase isozymes, but acclimation to low temperature increases alcohol dehydrogenase activity in the white part of the myotome.

The research described in this paper was supported by a grant from the Royal Dutch Academy of Sciences to A. van Waarde.

References

- BERGMEYER, H. U. (1970). *Methoden der Enzymatischen Analyse*. Weinheim: Verlag Chemie.
- CAMERON, J. N. AND KORMANIK, G. A. (1982). Intracellular and extracellular acid-base status as a function of temperature in the channel catfish, *Ictalurus punctatus*. *J. exp. Biol.* **99**, 127–142.
- HOCHACHKA, P. W. (1982). Metabolic arrest as a mechanism of protection against hypoxia. In *Protection of Tissues Against Hypoxia* (ed. A. Wauquier, M. Borgers and W. K. Amery). Amsterdam: Elsevier/North Holland Biomedical Press.
- HOCHACHKA, P. W. (1985). Assessing metabolic strategies for surviving O_2 -lack: role of metabolic arrest coupled with channel arrest. *Molec. Physiol.* **8**, 331–350.
- HOCHACHKA, P. W. AND GUPPY, M. (1987). *Metabolic Arrest and the Control of Biological Time*. Cambridge, MA: Harvard University Press.
- HOLOPAINEN, I. J. AND HYVÄRINEN, H. (1985). Ecology and physiology of crucian carp (*Carassius carassius* (L.)) in small Finnish ponds with anoxic conditions in winter. *Verh. int. Verein. Limnol.* **22**, 2566–2570.
- MOURIK, J., RAEVEN, P., STEUR, K. AND ADDINK, A. (1982). Anaerobic metabolism of red skeletal muscle of goldfish, *Carassius auratus* (L.): Mitochondrial produced acetaldehyde as anaerobic electron acceptor. *FEBS Lett.* **137**, 111–114.
- PIIRONEN, J. AND HOLOPAINEN, I. J. (1986). A note on seasonality in anoxia tolerance of crucian carp (*Carassius carassius* (L.)) in the laboratory. *Ann. Zool. Fenn.* **23**, 335–338.
- PÖRTNER, H. O. (1987). Contributions of anaerobic metabolism to pH regulation in animal tissues: theory. *J. exp. Biol.* **131**, 69–87.
- SHOUBRIDGE, E. A. AND HOCHACHKA, P. W. (1980). Ethanol: Novel end product of vertebrate anaerobic metabolism. *Science* **209**, 308–309.
- VAN DEN THILLART, G. (1977). Influence of oxygen availability on the energy metabolism of goldfish, *Carassius auratus* (L.) DSc thesis, Leiden University.
- VAN DEN THILLART, G. AND KESBEKE, F. (1977). Anaerobic production of carbon dioxide and ammonia by goldfish, *Carassius auratus* (L.) *Comp. Biochem. Physiol.* **59A**, 393–400.
- VAN DEN THILLART, G., KÖRNER, F., VAN WAARDE, A., ERKELENS, C. AND LUGTENBURG, J. (1989a). A flow-through probe for *in vivo* ^{31}P -NMR spectroscopy of unanesthetized aquatic vertebrates at 9.4 Tesla. *J. magn. Reson.* **84**, 573–579.
- VAN DEN THILLART, G., VAN BERGE HENEGOUWEN, M. AND KESBEKE, F. (1983). Anaerobic metabolism of goldfish, *Carassius auratus* (L.): Ethanol and CO_2 excretion rates and anoxia tolerance at 20, 10 and 5°C. *Comp. Biochem. Physiol.* **76A**, 295–300.

- VAN DEN THILLART, G. AND VAN WAARDE, A. (1991). pH-changes in fish during environmental anoxia and recovery: the advantages of the ethanol pathway. In *Physiological Strategies for Gas Exchange and Metabolism* (ed. A. J. Woakes, M. K. Grieshaber and C. R. Bridges), (*Soc. exp. Biol. Sem. Ser. no. 41*), pp. 173–190. Cambridge: Cambridge University Press.
- VAN DEN THILLART, G., VAN WAARDE, A., DOBBE, F. AND KESBEKE, F. (1982). Anaerobic energy metabolism of goldfish, *Carassius auratus* (L.): Effects of anoxia on the measured and calculated NAD⁺/NADH ratios in muscle and liver. *J. comp. Physiol.* **146**, 41–49.
- VAN DEN THILLART, G., VAN WAARDE, A., MULLER, H. J., ERKELENS, C., ADDINK, A. AND LUGTENBURG, J. (1989*b*). Fish muscle energy metabolism measured by *in vivo* ³¹P-NMR during anoxia and recovery. *Am. J. Physiol.* **256**, R922–R929.
- VAN DEN THILLART, G., VAN WAARDE, A., MULLER, H. J., ERKELENS, C. AND LUGTENBURG, J. (1990). Determination of high-energy phosphate compounds in fish muscle: ³¹P-NMR spectroscopy and enzymatic methods. *Comp. Biochem. Physiol.* **95B**, 789–795.
- VAN WAARDE, A. (1983). Aerobic and anaerobic ammonia production by fish. *Comp. Biochem. Physiol.* **74B**, 675–684.
- VAN WAARDE, A. (1988). Biochemistry of non-protein nitrogenous compounds in fish including the use of amino acids for anaerobic energy production. *Comp. Biochem. Physiol.* **91B**, 207–228.
- VAN WAARDE, A. (1991). Alcoholic fermentation in multicellular organisms. *Physiol. Zool.* (in press).
- VAN WAARDE, A., VAN DEN THILLART, G., ERKELENS, C., ADDINK, A. AND LUGTENBURG, J. (1990). Functional coupling of glycolysis and phosphocreatine utilization in anoxic fish muscle: An *in vivo* ³¹P-NMR study. *J. biol. Chem.* **265**, 914–923.
- VAN WAVERSVELD, J., ADDINK, A. AND VAN DEN THILLART, G. (1989*a*). Simultaneous direct and indirect calorimetry on normoxic and anoxic goldfish. *J. exp. Biol.* **142**, 325–335.
- VAN WAVERSVELD, J., ADDINK, A. AND VAN DEN THILLART, G. (1989*b*). The anaerobic energy metabolism of goldfish measured by simultaneous direct and indirect calorimetry during anoxia and hypoxia. *J. comp. Physiol.* **159**, 263–268.
- VAN WAVERSVELD, J., ADDINK, A., VAN DEN THILLART, G. AND SMIT, H. (1988). Direct calorimetry on free swimming goldfish at different oxygen levels. *J. therm. Anal.* **33**, 1019–1026.
- WALKER, R. M. AND JOHANSEN, P. H. (1977). Anaerobic metabolism of goldfish. *Can. J. Zool.* **55**, 1304–1311.
- WILLIAMSON, D. H., LUND, P. AND KREBS, H. A. (1967). The redox state of free nicotinamide adenine dinucleotide in the cytoplasm and mitochondria of rat liver. *Biochem. J.* **103**, 514–527.
- YEAGER, D. P. AND ULTSCH, G. R. (1989). Physiological regulation and conformation: A BASIC program for the determination of critical points. *Physiol. Zool.* **62**, 888–907.

